ACS SENSORS

Article

pubs.acs.org/acssensors

Peptide Functionalized Gold Nanoparticles with Optimized Particle Size and Concentration for Colorimetric Assay Development: Detection of Cardiac Troponin I

Xiaohu Liu,[†,‡,∥] Yi Wang,[†,§,∥] Peng Chen,[†] Austin McCadden,[†] Alagappan Palaniappan,[†] Jinling Zhang,[†] and Bo Liedberg*[,†]

[†]Centre for Biomimetic Sensor Science, School of Materials Science and Engineering, Nanyang Technological University, 50 Nanyang Drive, 637553 Singapore

[‡]School of Biological Sciences, Nanyang Technological University, 50 Nanyang Avenue, 639798 Singapore

[§]Wenzhou Institute of Biomaterials and Engineering, Chinese Academy of Sciences, Wenzhou, Zhejiang, 325001 China

Supporting Information

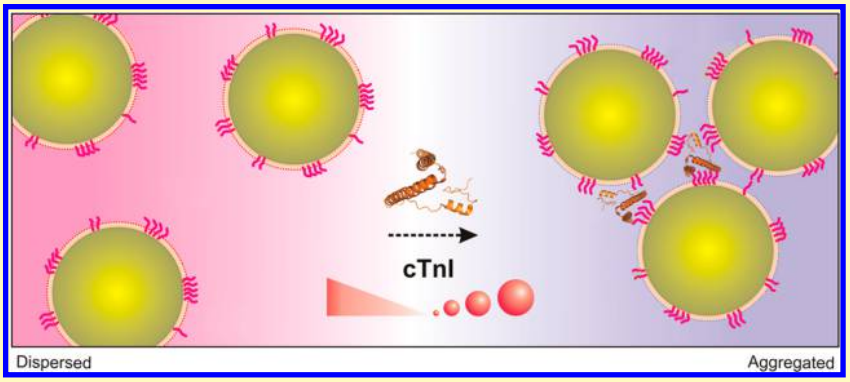

ABSTRACT: Peptide-functionalized gold nanoparticles (AuNPs) are extensively utilized in colorimetric assays for rapid and sensitive detection of various biomedical and environmental targets. Although extensively used as colorimetric reporting systems, the role of the size and concentration of the AuNPs has not been thoroughly investigated. In this study, a 12-mer cardiac troponin I (cTnI)-specific peptide CALNN-Peg_4-FYSHSFHENWPS was immobilized on AuNPs of different size and concentration via the CALNN anchoring sequence. A relationship was established between the total surface area of the AuNPs (binding availability) and response (centroid shift). Moreover, a colorimetric assay for cTnI operating under optimized conditions (36 nm AuNPs) yielded a limit of detection of 0.2 ng/mL (8.4 pM) when tested in diluted serum samples with an assay time of 10 min. This encouraging result opens up for further development of AuNP assays in early diagnosis of cardiac injury.

KEYWORDS: *peptide-functionalized gold nanoparticles, colorimetric sensing, cardiac troponin I, concentration of AuNPs, size of AuNPs*

Peptide-functionalized gold nanoparticles (AuNPs) recently have been extensively employed in biosensing.[1] The unique optical properties of AuNPs offer possibilities to transduce molecular interactions into detectable colorimetric signals that can be recorded by mobile "ubiquitous" technologies[2] and sometimes even by the naked eye.[1b] Peptides as alternative candidates in molecular affinity recognition offer several advantages over commonly used antibodies primarily because they are (1) easy to produce at high purity and (2) more robust.[3] In addition, they also provide an enormous flexibility and versatility with respect to structural and chemical properties.[4] Therefore, peptide-functionalized AuNPs offer a robust and viable route for developing rapid and sensitive colorimetric assays.[4,5] Although promising there are still very few systematic studies reported in the literature on how the AuNP size and concentration influences the assay performance (e.g., sensitivity and limit of detection etc.). Such information would certainly provide useful guidelines for the design of novel assays based on plasmonic nanoparticles. Herein we employ an established biomarker for cardiac injury to investigate the role of AuNP size and concentration on the overall assay performance in complex fluids.

Acute myocardial infarction (AMI) is one of the leading causes of morbidity and mortality in many developed countries across the world. There are several clinical biomarkers commonly involved in early detection of cardiac injury

Received: August 10, 2016
Accepted: November 10, 2016
Published: November 10, 2016

DOI: 10.1021/acssensors.6b00493
ACS Sens. 2016, 1, 1416−1422

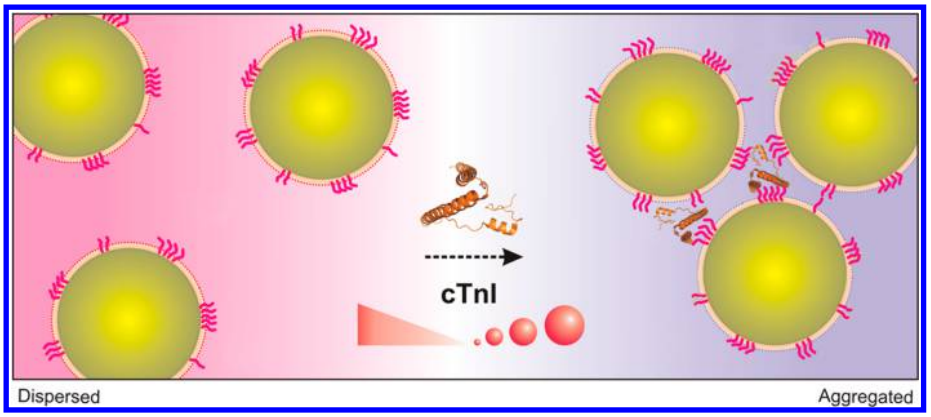

Figure 1. Schematic illustration of the AuNP-based assay for detection of cTnI using AuNPs of different size and concentration. In the absence of cTnI, the AuNPs display an excellent colloidal stability and remain dispersed (left, red). Addition of cTnI causes massive aggregation and a concomitant colorimetric change in a concentration-dependent manner (right, purple).

including the MB isoenzyme of creatine kinase (CK-MB), and myoglobin.[6] As one of the biomarkers, cardiac troponin I (cTnI), existing in a 3-unit complex (I, C, and T) located on actin filament is a key regulator of cardiac muscle contraction. It has been intensively studied as a principle biomarker for diagnosis of AMI due to its excellent specificity and sensitivity.[7] Once the myocardiac damage occurs, the level of cTnI in serum rapidly increases within 3−4 h and keeps increasing in following several days which offers an extended diagnostic period of AMI with elevated levels of cTnI.[7b,8] Commonly used techniques for AMI diagnostics are enzyme-linked immunosorbent assay (ELISA) and radioimmunoassay (RIA).[9] More recently, electrochemical, fluorescence and surface plasmon resonance assays have been proposed.[10] Although they address some of the apparent problems in ELISA and RIA such as long assay time, multistep processing, radioactive waste handling and high overall cost, they require sophisticated instrumentation and often rely delicate/fragile recognition entities like antibodies. As a result, it is difficult to apply those assays in less developed and remote areas where diagnosis of AMI is urgently needed.

In this contribution we report on a peptide-functionalized AuNP-based colorimetric model assay for cTnI in serum samples. Briefly, a 12-mer synthetic peptide receptor with nanomolar binding affinity to cTnI, which has been reported by Banta's group using a polyvalent phage displayed library,[11] was immobilized onto AuNPs via the cysteine residue. As the peptide can bind to multiple epitopes on cTnI, it offers a convenient strategy to aggregate AuNPs (Figure 1). AuNPs of varying size and concentration were employed to optimize sensitivity and limit of detection, which would be crucial for future assay development.

MATERIAL AND METHODS

Materials. The peptide binder TP (CALNN-PEG_4-FYSHSFHENWPS) and peptide spacer (CALNN) used were customized and purchased from GL, Shanghai. Cardiac Troponin I was obtained from Abcam, US. All other chemicals were purchased from Sigma-Aldrich and used as received.

Synthesis of AuNPs. The small gold nanoparticles (d = 6 nm) were synthesized as follows: 0.5 mL of 0.1 M gold(III) chloride trihydrate solution and 2 mL of 0.025 M sodium citrate solution were mixed into 187.5 mL of Milli-Q water and stirred, followed by addition of 5 mL of freshly prepared 0.1 M $NaBH_4$. Subsequent color change was observed from colorless to orange. Stirring was then stopped and the solution was left undisturbed for 2 h. The 16, 25, and 36 nm gold nanoparticles were synthesized by citrate reduction method. Briefly, 100 mL of 0.01% (0.1 mg/mL) gold(III) chloride trihydrate solution was boiled in a well-cleaned flask. After that, 10 mg/mL sodium citrate was added to the gold salt solutions (2.75, 2, and 1.75 mL) in order to obtain 16, 25, and 36 nm AuNPs, respectively. The solution then changed color from light yellow to red and was kept boiling for another 30 min. The synthesized spherical gold nanoparticles were verified by dynamic light scattering (DLS; Zetasizer Nano S, Malvern, U.K.) and stored in fridge until use.

Preparation of TP Functionalized on Planar Gold Thin Films and AuNPs. Planar gold substrate was functionalized with TP and thiol-PEG_6-OH in different ratios (10%, 30%, 50%, and 100%) with the total concentration at 1 mM. The cleaned bare gold substrates were immersed in the mixed TP/thiol-PEG_6-OH ethanol solutions and incubated overnight. Then the substrates were rinsed with ethanol/water and immediately installed in SPR setup for testing.

For the AuNP experiments, 12.5 μL of the peptide (CALNN) spacer (2 mM) and 25 μL of TP (1 mM) were mixed in 500 μL phosphate buffered saline buffer (1×, 0.05% Tween) followed by adding of 1 mL AuNPs (6 nm, 16 nm, 25 or 36 nm). The AuNPs solutions were left overnight. The 6 nm functionalized AuNPs were concentrated in Vivaspin 30 kDa tubes, while 16 and 25 nm functionalized AuNPs were concentrated by centrifugation. All of the particles went through a column for purification (PD MiniTrap G-25) except for the large 36 nm functionalized AuNPs which were purified repeatedly by centrifugations. All the functionalized AuNPs were stored in fridge until use.

SPR Test for cTnI Binding. The SPR measurement was undertaken using a home-built SPR setup described in our previous work.[12] Briefly, A transverse magnetically (TM, p-polarization) polarized beam from a HeNe laser (λ = 632.8 nm) was coupled to a LASFN9 glass prism for the excitation of LSP (localized surface plasmon) and PSP (propagating surface plasmon). Onto the prism base, a sensor chip with a structure supporting surface plasmon was optically matched with matching oil (n = 1.700, Cargille Labs, Cedar Grove, NJ). Aqueous samples (with a refractive index close to n_b = 1.333) were pumped at the flow rate of 0.4 mL min^{-1} through the flow-cell using a peristaltic pump. The analyzed samples circulated in the fluidic system with a total volume of 800 μL. The LASFN9 glass prism was mounted on a motorized rotation stage and angular reflectivity spectra R(Θ) were measured by using a photodiode detector and lock-in amplifier. In the kinetic mode, PBS (1 × , Tween 0.05%) was running through for 30 min to stabilize the surface. Then cTnI of 1 μg/mL was injected into the chamber and the reflectivity was recorded over time to determine on- and off rate constants and affinity at an incident angle close to the resonant angle. Details on the fitting of the association and dissociation constants can be found in the Supporting Information.

Measurements of Centroid Shift. Each of the functionalized AuNP samples were loaded in the Insplorion XNano (Insplorion,

DOI: 10.1021/acssensors.6b00493
ACS Sens. 2016, 1, 1416−1422

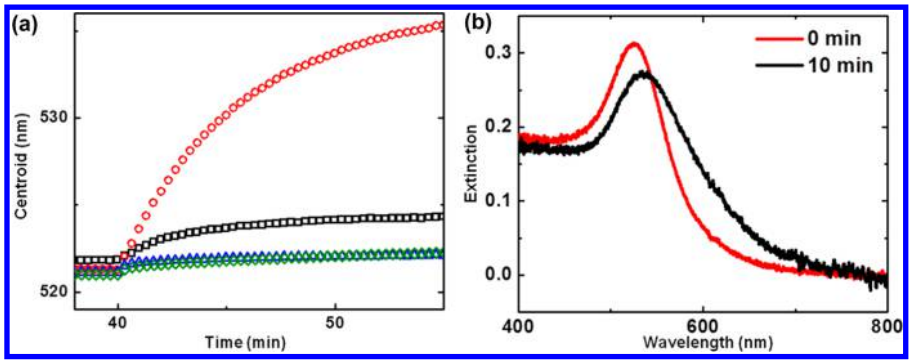

Figure 2. (a) Kinetic measurements (centroid shift) upon addition of cTnI (1 μg/mL) in buffer to unmodified AuNPs (green diamond), TP_{50}-AuNPs (red circle), and TP_{100}-AuNPs (black squares). Also shown is the kinetic data for TP_{50}-AuNPs in ×100 times diluted serum (blue triangle). (b) Extinction spectra of TP_{50}-AuNPs before 0 and 10 min after addition of 1 μg/mL cTnI.

Sweden). A stable baseline (extinction mode) was obtained after 10 min. Different concentrations of 2 μL of cTnI were then added to 200 μL AuNPs samples and kinetic data (centroid shifts[13]) were recorded along with their spectra. In the rabbit serum tests, rabbit serum was first mixed with various concentrations of cTnI in 1:1 volume ratio, followed by adding 2 μL of mixture into 200 μL AuNP solutions. The final dilution of rabbit serum was therefore 200 times.

RESULTS AND DISCUSSION

Peptide Binder for cTnI. The peptide binder (TP) for cTnI contains a 5-mer sequence at the N-terminus (CALNN) that is used as an anchor to the AuNPs.[14] This short peptide segment is used to lift the recognition sequence of (TP) from the surface to provide a better presentation to the target (cTnI). CALNN alone also offers protection against nonspecific binding in complex fluids and contributes to an improved colloidal stability of the AuNP suspension. Furthermore, AuNPs coated with CALNN are also robust and resistant to high salt concentrations.[14] The AuNPs could be subsequently purified in gel columns instead of repeated centrifugations that simplified the purification process. Besides improving the colloidal stability, the short peptide also could be used as a mixing agent with TP to control the receptor distribution on the AuNPs. In our case, the recognition sequence was attached to the end of the CALNN peptide via a 4-mer PEG spacer. The TP peptide sequence had been screened using the polyvalent phage display method[23] and it displayed nanomolar-affinity when attached to the phage particles. Although the binding site was not identified, it became evident that it could bind to multiple epitopes on a single cTnI molecule.[11,15]

Preoptimization of Peptide Functionalization. Complementary surface plasmon resonance (SPR) experiments on planar gold were undertaken to explore the importance of receptor (TP) distribution on the surface. Planar gold films were modified with TP at 4 different solution compositions from 10% to 100% using a thiol-PEG_6−OH as mixing agent. Interestingly, the SPR response was substantially higher for the surface modified with 50% TP than for those prepared from solutions containing 10, 30, and 100% TP, respectively (Figure S1). These experiments suggest that both reception concentration and accessibility determines the affinity binding between cTnI and the peptide and encouraged us to explore different mixtures for the homogeneous AuNP assay.

Control experiments using unmodified AuNPs (25 nm) revealed a minor shift from 521 to 522.5 nm when 1 μg/mL cTnI was added (green diamond, Figure 2a). Moreover, the AuNPs remained dispersed overnight suggesting that addition of cTnI to unmodified AuNPs did not induce any aggregation. A similar shift was seen when a TP_{50}-AuNP solution was added to a suspension of 100 times diluted serum which we attributed to protein adsorption on the AuNP surface (blue triangle, Figure 2a). In contrast, AuNPs coated with 50% TP (TP_{50}-AuNPs) and 100% TP (TP_{100}-AuNPs) displayed significant centroid shifts upon addition of 1 μg/mL cTnI for 10 min (see red circle and black square respectively, Figure 2a). Moreover, the AuNPs precipitated to the bottom of the test tube after a few hours. The TP_{50}-AuNPs showed the largest centroid peak shift and an overall intensity decrease and broadening was seen after incubation with cTnI (Figure 2b). For example, TP_{50}-AuNPs showed a centroid shift 16 nm whereas the corresponding shift for TP_{100}-AuNPs was only 2.5 nm findings that are in line with the SPR experiments on planar gold films (see Supporting Information, Figure S1). Therefore, AuNPs with 50% TP was chosen in the following set of experiments.

In the homogeneous AuNP assay, the particles aggregated in about 10 min after the addition of cTnI. This process is substantially faster than the time required to reach equilibrium adsorption on the planar gold surface (Figure S1). The reason could be attributed to differences in the surface modification strategies used as well as to variations in the reaction kinetics in homogeneous solution and on the planar surface (effect of curvature) and mass transport limitations.[16]

In the case of AuNP assays, charged molecules are preferred to ensure excellent colloidal stability. In this study, the short peptide (CALNN), terminated with a carboxylic acid group (COOH) was used as capping agent to stabilize the AuNP suspension. With the positively charged cTnI (pI = 9.87), the binding rate between the functionalized particles and cTnI is expected increase because of electrostatic attraction. Additionally, negatively charged AuNPs is also expected to result in reduced nonspecific absorption in serum because the majority of the serum proteins (e.g., HSA) are negatively charged at neutral pH (Figure 2a).[17]

Size- and Concentration-Dependent Sensitivity. Most of the AuNP-based colorimetric assays reported thus far in the literature have utilized AuNPs with a size from 13 to 40 nm in diameter. Although the sensitivity is known to depend on the particle size and concentration, there are essentially no systematic studies focusing on how these parameters influence the overall sensor performance. In our assay of cTnI, AuNPs with diameters of 6, 16, 25, and 36 nm (Figure S2) were employed to investigate the influence of AuNP size on the sensitivity and limit of detection (LOD). Moreover, four

DOI: 10.1021/acssensors.6b00493
ACS Sens. 2016, 1, 1416−1422

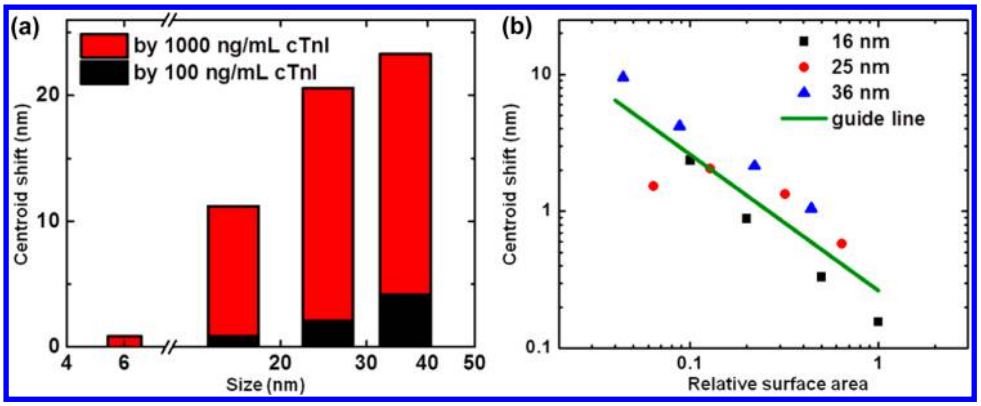

Figure 3. (a) Centroid shifts obtained upon addition of cTnI (100 and 1000 ng/mL) to different sizes of TP_{50}-AuNPs at a dilution factor of 5. (b) Centroid shifts plotted for different relative surface areas of AuNPs (16 nm, black square; 25 nm, red circle; and 36 nm, blue triangle) in response to 100 ng/mL cTnI. The data points in (b) represent samples of increasing dilution factor (from right to left).

different concentrations with dilution factors of 1, 2, 5, and 10 were examined, where a dilution factor of 1 refers to the highest concentration of AuNPs (Figure S3a).

The centroid shifts for AuNPs of different sizes are plotted in Figure 3a. For example, the 6 nm AuNPs induced a small centroid shift of ~1.5 nm upon incubation with 1 μg/mL cTnI, whereas the 36 nm AuNPs induced a centroid shift of 23 nm (Figure 3a). At lower concentration of cTnI (100 ng/mL), a similar trend is observed, but the centroid shifts for all sizes of AuNPs were less than 5 nm (Figure 3a). DLS experiments of samples exposed to 100 ng/mL cTnI indicated that the peak shift was ascribed to the aggregation of AuNPs. For example, the size of 36 nm AuNP increased up to ~120 nm after 11 min incubation in cTnI (Figure S3b and S3c).

To account for both size and concentration of AuNPs on the sensitivity, we introduced the surface area of the nanoparticles as a key parameter. The surface area and concentration of different nanoparticles were calculated based on the amount of gold precursor used during the synthesis (Table 1). The larger nanoparticles typically provided lower total surface area.

Table 1. Relative Surface Area and Concentration of AuNPs with Different Diameters

particle size d/nm	6[a]	16	25	36
relative surface area (w.r.t. 16 nm AuNPs)	27	1.0	0.65	0.44
concn (nM) of AuNPs with dilution factor of 1	38	0.20	0.053	0.018

[a]Initial concentration of gold salt used in synthesis of 6 nm AuNPs was 10 times higher than the others.

The centroid shifts for the three largest particles were found to be inversely proportional to the relative surface area of the AuNPs (Figure 3b). Thus, AuNPs possessing small surface areas (large particles) should preferably be used to boost the response at low concentrations of the analyte (Figure 3b). We reason that the aggregation of AuNPs most likely is determined by the number of cTnI binding sites on the surface of the AuNPs. Therefore, in order to improve the sensor response (i.e., to initiate the aggregation with less amount of analyte) large AuNPs and high dilution factors would be advantageous.

Detection of cTnI. Typically, the LOD of a sensor is determined both by the sensor response and the noise level. All four concentrations of the 36 nm AuNPs (dilution factor: 10, 5, 2, and 1) were used for the detection of cTnI. Among them, the most diluted AuNPs (dilution factor 10) gave rise to the most significant response followed by 5 and 2, while the one with dilution factor of 1 only showed minor centroid shifts throughout the series of cTnI concentrations (Figure 4a), in line with hypothesis above. In addition, the color change was clearly observed (inset, Figure 4a). The most diluted AuNPs, however, displayed the highest noise in our system because of the low absorbance values and led to the worst LOD 1.53 ng/mL (black square, Figure 4b). The best LOD of 0.43 ng/mL was estimated from AuNPs at a dilution factor of 1 although its response was the lowest. We ascribed this to the low noise level (green diamond, Figure 4b). The AuNPs with dilution factor of 2 and 5 provided a LOD of 0.59 and 0.98 ng/mL, respectively (blue triangle and red circle, Figure 4b).

Other sizes of AuNPs were also investigated (Figure S4a 16 nm AuNPs and Figure S4b 25 nm AuNPs). Figure 4c shows essentially the similar LOD for the 25 and 36 nm (average LOD = 1.10 and 0.88 ng/mL, respectively). In contrast, the 16 nm AuNPs resulted in significantly higher LOD values (average LOD = 10 ng/mL). These results indicate that large AuNPs at high concentration provide relatively better LOD despite their low response. With particles size of 25 and 36 nm, the LOD is approximately inversely proportional to the relative surface area of the AuNPs (Figure 4c). This is because at low concentration of analyte the surface area of AuNPs has negligible effect to the sensor response. The LOD is therefore mainly affected by the noise level (N), which is inversely proportional to the absorption A of the AuNPs solution,[18] given as

$$A = (n_{Au}\pi r^2 Q_{extt} L/4\ln 10) \quad (1)$$

where Q_{ext} and L are the extinction efficiency and optical path length, respectively. n_{Au} and r are the number and the radius of AuNPs, respectively, and the surface area of the AuNPs is equal to $4n_{Au}\pi r^2$. Thus, the noise level is inversely proportional to the relative surface area and proportional to the dilution factor of AuNPs, which is consistent with the experimental results as indicated in Figure 4b.

The assay was conducted in rabbit serum (× 200 diluted) spiked with various concentrations of cTnI to investigate the feasibility and sensitivity on the detection of cTnI in a complex matrix. A control experiment was carried out in ×200 diluted serum sample without spiking of cTnI to achieve a baseline (black curve in Figure 5a). Again, the response (centroid shift of 1.3 nm) was ascribed to the nonspecific adsorption of proteins in serum onto the surface of the AuNPs. The serum sample spiked with cTnI led to increasing centroid shifts with

DOI: 10.1021/acssensors.6b00493
ACS Sens. 2016, 1, 1416−1422

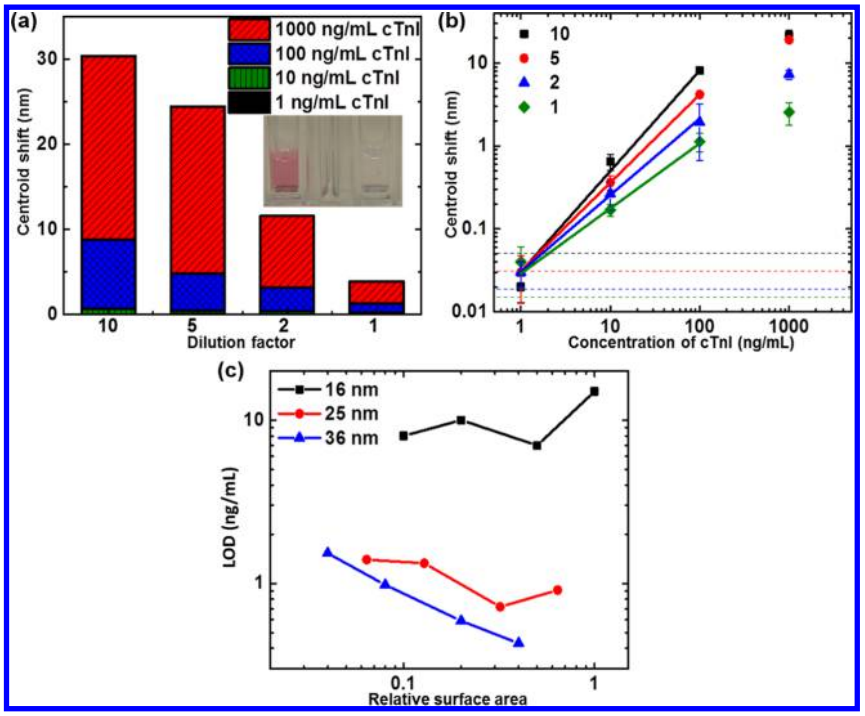

Figure 4. (a) Centroid shifts of 36 nm TP_{50}-AuNPs with all dilution factors exposed to series concentrations of cTnI. Inset: photograph of color change comparing the control without cTnI (left side) and sample with 1 μg/mL cTnI (dilution factor: 2). (b) Fitted calibration curves of centroid shifts obtained from 36 nm TP_{50}-AuNPs for cTnI detection with all dilution factors: 10 (black square), 5 (red circle), 2 (blue triangle), and 1 (green diamond). (c) LODs calculated for cTnI by 16 nm (black square), 25 nm (red circle), and 36 nm (blue triangle) TP_{50}-AuNPs at various AuNPs concentrations normalized by relative surface area. The data points in (c) represent increasing dilution factor (from right to left).

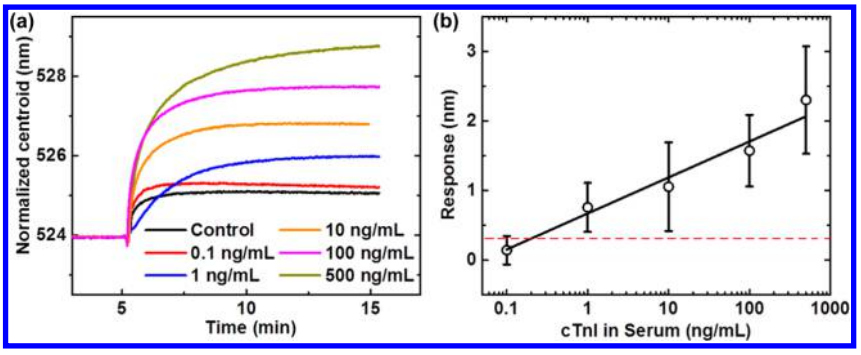

Figure 5. (a) Kinetic responses of centroid shifts for different concentrations of cTnI in serum. (b) Fitted calibration curve of centroid shifts obtained from 36 nm TP_{50}-AuNPs for detection of cTnI in ×200 times diluted serum.

increasing concentration of the target. As shown in Figure 5a, centroid shifts from 1.5 nm up to 4.5 nm was observed at cTnI concentration from 0.1 ng/mL to 500 ng/mL in serum. These findings indicate that the proposed assay is feasible for the detection of cTnI at concentrations down to 0.1 ng/mL in serum. However, the assay did not work when the serum was mixed with TP_{50}-AuNP prior to exposure of serum spiked with cTnI. As illustrated in Figure S5a, when the TP_{50}-AuNP sample was first incubated with plain serum for 10 min, followed by addition of cTnI (500 ng/mL) no obvious response was observed. This somewhat unexpected result is ascribed to blocking of the peptide binding sites by serum proteins (typically a few hundred μg/mL). In the case of exposure of cTnI spiked in serum, cTnI competes with serum proteins for the binding on AuNPs. As a result, a clear enhanced centroid shift could be identified. The response was about 2 to 4 folds lower than that in buffer with high concentrations of cTnI such as 100 ng/mL. The calibration curve in Figure 5b points toward an LOD of 0.20 ng/mL for cTnI in serum with an assay time of 10 min. The noise level (dashed line in Figure 5b) was determined as three times of the standard deviation of the response for a blank (nonspiked) serum sample. This LOD is very encouraging for the potential use of peptide-conjugated AuNPs as a quick and accurate assay for cTnI. It performed successfully for the detection of cTnI in serum sample with LOD comparable to cTnI detection in buffer. Moreover, the obtained LOD is about 10 to 100 folder lower than our previously reported method based on electrofocusing enhanced localized surface plasmon resonance biosensor for cTnI detection.[3b] It is expected that the LOD for the detection of cTnI in serum can be further optimized in near future to meet the clinical requirements,[19] e.g., by improving the affinity of the receptor and by pretreating the serum sample and optimizing the surface chemistry of the AuNPs to minimize the nonspecific adsorption and interferences.

DOI: 10.1021/acssensors.6b00493
ACS Sens. 2016, 1, 1416−1422

CONCLUSION

Peptides as recognition elements are attractive candidates in biomolecular recognition as they offer tunable sensitivity and selectivity along with substantially improved robustness as compared to antibodies. In combination with AuNPs, they offer a promising route for developing fast, simple, and accurate assays for a broad spectrum of targets. As described herein by using a prescreened peptide binder for cTnI, a colorimetric assay involving peptide-functionalized AuNPs was successfully developed. The size and concentration of AuNPs were optimized to boost the LOD, and the response (centroid peak shift) was found to be inversely proportional to the surface area of the AuNPs. Moreover, a LOD down to 0.20 ng/mL could be achieved by using large AuNPs (36 nm) with dilution factor of 2 in rabbit serum. The assay time is about 10 min which enables semicontinuous monitoring of cTnI levels during the critical hours of disease development.[20] Moreover, the colorimetric responses and the encouraging performance of the assay in real samples will undoubtedly facilitate further development into a user-friendly assay format.

ASSOCIATED CONTENT

Supporting Information

The Supporting Information is available free of charge on the ACS Publications website at DOI: 10.1021/acssensors.6b00493.

SPR test of cTnI binding responses to different gold substrate functionalized with different ratios; DLS verification of aggregate sizes of AuNPs of varying size; photograph of various concentrations of AuNPs; calibration and kinetic measurements (PDF)

AUTHOR INFORMATION

Corresponding Author

*E-mail: bliedberg@ntu.edu.sg.

Author Contributions

‖X.L. and Y.W. contributed equally to this work.

Notes

The authors declare no competing financial interest.

ACKNOWLEDGMENTS

The authors are thankful for the financial support from Science & Engineering Research Council (SERC) of Agency for Science, Technology and Research (A*STAR), for projects under the Number 102 152 0015. The project was also supported by MOE-2014-T1-001-133, Singapore and from the government of Wenzhou, China for the startup fund WIBEZD2014004-02.

REFERENCES

(1) (a) Rosi, N. L.; Mirkin, C. A. Nanostructures in biodiagnostics. *Chem. Rev.* **2005**, *105* (4), 1547−62. (b) Aili, D.; Stevens, M. M. Bioresponsive peptide-inorganic hybrid nanomaterials. *Chem. Soc. Rev.* **2010**, *39* (9), 3358−3370.

(2) Wang, Y.; Liu, X.; Chen, P.; Tran, N. T.; Zhang, J.; Chia, W. S.; Boujday, S.; Liedberg, B. Smartphone spectrometer for colorimetric biosensing. *Analyst* **2016**, *141* (11), 3233−8.

(3) (a) Chen, H.; Huang, J.; Palaniappan, A.; Wang, Y.; Liedberg, B.; Platt, M.; Tok, A. I. A review on electronic bio-sensing approaches based on non-antibody recognition elements. *Analyst* **2016**, *141* (8), 2335−46. (b) Zhang, J.; Wang, Y.; Wong, T. I.; Liu, X.; Zhou, X.; Liedberg, B. Electrofocusing-enhanced localized surface plasmon resonance biosensors. *Nanoscale* **2015**, *7* (41), 17244−8.

(4) (a) Gao, L.; Liu, M.; Ma, G.; Wang, Y.; Zhao, L.; Yuan, Q.; Gao, F.; Liu, R.; Zhai, J.; Chai, Z.; et al. Peptide-conjugated gold nanoprobe: intrinsic nanozyme-linked immunsorbant assay of integrin expression level on cell membrane. *ACS Nano* **2015**, *9* (11), 10979−10990. (b) Guarise, C.; Pasquato, L.; De Filippis, V.; Scrimin, P. Gold nanoparticles-based protease assay. *Proc. Natl. Acad. Sci. U. S. A.* **2006**, *103* (11), 3978−3982.

(5) (a) Chen, P.; Selegård, R.; Aili, D.; Liedberg, B. Peptide Functionalized Gold Nanoparticles for Colorimetric Detection of Matrilysin (MMP-7) Activity. *Nanoscale* **2013**, *5*, 8973−8976. (b) Aili, D.; Selegård, R.; Baltzer, L.; Enander, K.; Liedberg, B. Colorimetric Protein Sensing by Controlled Assembly of Gold Nanoparticles Functionalized with Synthetic Receptors. *Small* **2009**, *5* (21), 2445−2452. (c) Chandrawati, R.; Stevens, M. M. Controlled assembly of peptide-functionalized gold nanoparticles for label-free detection of blood coagulation Factor XIII activity. *Chem. Commun.* **2014**, *50* (41), 5431−5434.

(6) (a) Apple, F. S.; Jaffe, A. S. Bedside multimarker testing for risk stratification in chest pain units: The chest pain evaluation by creatine kinase-MB, myoglobin, and troponin I (CHECKMATE) study. *Circulation* **2001**, *104* (22), E125−E126. (b) Howie-Esquivel, J.; White, M. Biomarkers in acute cardiovascular disease. *Journal of cardiovascular nursing* **2008**, *23* (2), 124−31.

(7) (a) Adams, J. E., 3rd; Bodor, G. S.; Davila-Roman, V. G.; Delmez, J. A.; Apple, F. S.; Ladenson, J. H.; Jaffe, A. S. Cardiac troponin I. A marker with high specificity for cardiac injury. *Circulation* **1993**, *88* (1), 101−6. (b) Babuin, L.; Jaffe, A. S. Troponin: the biomarker of choice for the detection of cardiac injury. *Can. Med. Assoc. J.* **2005**, *173* (10), 1191−1202.

(8) (a) Patil, H.; Vaidya, O.; Bogart, D. A Review of Causes and Systemic Approach to Cardiac Troponin Elevation. *Clin. Cardiol.* **2011**, *34* (12), 723−728. (b) Casals, G.; Filella, X.; Bedini, J. L. Evaluation of a new ultrasensitive assay for cardiac troponin I. *Clin. Biochem.* **2007**, *40* (18), 1406−1413. (c) Melanson, S. E.; Bonaca, M.; Scirica, B.; Sabatine, M.; Morrow, D. A.; Jarolim, P. Prospective evaluation of the prognostic implications of low level elevation of cardiac troponin using a new highly-sensitive assay for cardiac troponin I: Results from the MERLIN-TIMI 36 trial. *Clin. Chem.* **2008**, *54* (6), A77.

(9) (a) Collinson, P. O.; Boa, F. G.; Gaze, D. C. Measurement of cardiac troponins. *Ann. Clin. Biochem.* **2001**, *38*, 423−449. (b) Melanson, S. E. F.; Tanasijevic, M. J.; Jarolim, P. Cardiac troponin assays - A view from the clinical chemistry laboratory. *Circulation* **2007**, *116* (18), E501−E504.

(10) (a) Ko, S.; Kim, B.; Jo, S. S.; Oh, S. Y.; Park, J. K. Electrochemical detection of cardiac troponin I using a microchip with the surface-functionalized poly(dimethylsiloxane) channel. *Biosens. Bioelectron.* **2007**, *23* (1), 51−59. (b) Ahammad, A. J. S.; Choi, Y. H.; Koh, K.; Kim, J. H.; Lee, J. J.; Lee, M. Electrochemical Detection of Cardiac Biomarker Troponin I at Gold Nanoparticle-Modified ITO Electrode by Using Open Circuit Potential. *Int. J. Electrochem. Sci.* **2011**, *6* (6), 1906−1916. (c) Han, X.; Li, S.; Peng, Z.; Othman, A. M.; Leblanc, R. Recent Development of Cardiac Troponin I Detection. *ACS Sensors* **2016**, *1* (2), 106−114.

(11) Park, J. P.; Cropek, D. M.; Banta, S. High Affinity Peptides for the Recognition of the Heart Disease Biomarker Troponin I Identified Using Phage Display. *Biotechnol. Bioeng.* **2010**, *105* (4), 678−686.

(12) (a) Wang, Y.; Huang, C. J.; Jonas, U.; Wei, T.; Dostalek, J.; Knoll, W. Biosensor based on hydrogel optical waveguide spectroscopy. *Biosens. Bioelectron.* **2010**, *25* (7), 1663−8. (b) Wang, Y.; Brunsen, A.; Jonas, U.; Dostalek, J.; Knoll, W. Prostate specific antigen biosensor based on long range surface plasmon-enhanced fluorescence spectroscopy and dextran hydrogel binding matrix. *Anal. Chem.* **2009**, *81* (23), 9625−9632.

(13) Nusz, G. J.; Marinakos, S. M.; Curry, A. C.; Dahlin, A.; Hook, F.; Wax, A.; Chilkoti, A. Label-Free Plasmonic Detection of Biomolecular

DOI: 10.1021/acssensors.6b00493
ACS Sens. 2016, 1, 1416−1422

Binding by a Single Gold Nanorod. *Anal. Chem.* **2008**, *80* (4), 984−989.
(14) Levy, R.; Thanh, N. T. K.; Doty, R. C.; Hussain, I.; Nichols, R. J.; Schiffrin, D. J.; Brust, M.; Fernig, D. G. Rational and combinatorial design of peptide capping Ligands for gold nanoparticles. *J. Am. Chem. Soc.* **2004**, *126* (32), 10076−10084.
(15) Wu, J.; Cropek, D. M.; West, A. C.; Banta, S. Development of a Troponin I Biosensor Using a Peptide Obtained through Phage Display. *Anal. Chem.* **2010**, *82* (19), 8235−8243.
(16) Wang, Y.; Dostalek, J.; Knoll, W. Magnetic Nanoparticle-Enhanced Biosensor Based on Grating-Coupled Surface Plasmon Resonance. *Anal. Chem.* **2011**, *83* (16), 6202−6207.
(17) Pieper, R.; Gatlin, C. L.; Makusky, A. J.; Russo, P. S.; Schatz, C. R.; Miller, S. S.; Su, Q.; McGrath, A. M.; Estock, M. A.; Parmar, P. P.; Zhao, M.; Huang, S. T.; Zhou, J.; Wang, F.; Esquer-Blasco, R.; Anderson, N. L.; Taylor, J.; Steiner, S. The human serum proteome: Display of nearly 3700 chromatographically separated protein spots on two-dimensional electrophoresis gels and identification of 325 distinct proteins. *Proteomics* **2003**, *3* (7), 1345−1364.
(18) Chen, P.; Liedberg, B. Curvature of the Localized Surface Plasmon Resonance Peak. *Anal. Chem.* **2014**, *86* (15), 7399−7405.
(19) Sherwood, M. W.; Newby, L. K. High-sensitivity troponin assays: evidence, indications, and reasonable use. *J. Am. Heart Assoc.* **2014**, *3* (1), e000403.
(20) Mahajan, V. S.; Jarolim, P. How to Interpret Elevated Cardiac Troponin Levels. *Circulation* **2011**, *124* (21), 2350−2354.

DOI: 10.1021/acssensors.6b00493
ACS Sens. 2016, 1, 1416−1422